MULTIMODE STIMULATED RAMAN SCATTERING WITH SQUEEZED LIGHT

P. Král

Institute of Physics, Czechoslovak Acad. Sci., Na Slovance 2, 180 40 Praha 8, Czechoslovakia

Received 2 March 1990

Stimulated Raman scattering of a multimode pump light on an one-mode phonon system is examined. The pump light is expected to be strong, so that it can be treated classically. The phonon mode and scattered Stokes and anti-Stokes modes are described quantally. The phonon is prepared in a coherent state and the scattered modes are prepared in displaced and squeezed states at the input.

1. Introduction

Raman scattering has been investigated in a number of papers and on various media [1]. Considering the problem from the point of view of the quantum optics, we are interested in statistics of scattered Stokes and anti-Stokes modes [2]. The usual way consists in eliminating operators of a scattering medium and replacing the latter by effective interaction constants [3]. Such problems as spontaneous scattering should be examined quantally [4]. Unfortunately only very simple systems, described quantum mechanically, can be solved exactly. One of the exceptions is scattering on multilevel systems [5].

Brillouin scattering on one-phonon mode has been investigated in [6]. This model can be represented for example by the vibrating mode of a simple molecule, flying through a resonator on the analogy of Rydberg atoms. Another example is scattering on a reservoir having a discrete frequency spectrum, where modes pertaining to a single frequency can be considered as an effective single mode. This reservoir can really be prepared by confined optical phonon modes in a superlattice [7]. Such modes have a discrete energy structure. It arises due to the lack of cross sections of dispersion curves for optical phonon branches from the neighbouring materials, appearing in the alternating layers of a superlattice. This effect leads to confinement of optical phonon modes in every layer and to a resultant discrete energy structure, with the number of levels depending on the number of elementary cells in every layer. Modes from different layers have equivalent parameters and could be represented, from the view of a scattering on a thin layer, by a single mode with a corresponding interaction constant. If we use an intense pump light, which can be treated as a classical source without depletion, the scattering problem on the discrete energy structure will be decoupled and every energy level in such a scattering problem can be treated separately. If in addition we assume that the pump light is polychromatic, with nonoverlapping scattered modes, or at least if we assume two

different polarizations, we obtain a solvable problem, which will be treated here. (The coherence time should be longer than the time of observation due to the constant phase relations between different modes and due to the resonant approximation, which is independent of mode frequencies.) Polychromatic scattering appears often in experiments and it was studied in a number of works [8]. We consider stimulated scattering and prepare scattered Stokes and anti-Stokes modes in displaced and squeezed fields. The preparation of squeezed and strongly displaced fields has been suggested in [9]. Atomic transitions in a polychromatic squeezed vacuum have been investigated in [10].

The paper is organized as follows. In Sec. 2 we solve the Heisenberg equations for the Hamiltonian modelling the described problem. In Sec. 3 we find the complete antinormal and normal characteristic functions. Section 4 is devoted to the single-mode photon number generating functions $C_{\mathcal{N}}^{(w)}$ [11]. The end of that section shortly discusses the problem for cumulated modes. Numerical results in Sec. 5 demonstrate the case of the pump field with two modes. Conclusion closes the paper.

2. Solution of the Heisenberg equations

The Hamiltonian of the multimode Raman scattering with classical pumping, if losses have been neglected, reads

$$H = \hbar\omega_{\mathrm{v}} a_{\mathrm{v}}^{+} a_{\mathrm{v}} + \sum_{i} \hbar(\omega_{\mathrm{s}i} a_{\mathrm{s}i}^{+} a_{\mathrm{s}i} + \omega_{\mathrm{a}i} a_{\mathrm{a}i}^{+} a_{\mathrm{a}i}) + H_{\mathrm{int}} ,$$

$$H_{\mathrm{int}} = -\sum_{j} \hbar[g_{\mathrm{s}j} a_{\mathrm{s}j}^{+} a_{\mathrm{v}}^{+} \mathrm{e}^{-\mathrm{i}(\omega_{1j}t - \varphi_{1j})} + g_{\mathrm{s}j}^{*} a_{\mathrm{s}j} a_{\mathrm{v}} \mathrm{e}^{\mathrm{i}(\omega_{1j}t - \varphi_{1j})}$$

$$+ g_{\mathrm{a}j} a_{\mathrm{a}j}^{+} a_{\mathrm{v}} \mathrm{e}^{-\mathrm{i}(\omega_{1j}t - \varphi_{1j})} + g_{\mathrm{a}j}^{*} a_{\mathrm{a}j} a_{\mathrm{v}}^{+} \mathrm{e}^{\mathrm{i}(\omega_{1j}t - \varphi_{1j})}] . \tag{2.1}$$

Here $a_{\mathrm{s}j}^{+}$, $a_{\mathrm{s}j}$, $a_{\mathrm{a}j}^{+}$, $a_{\mathrm{a}j}$, and a_{v}^{+}, a_{v} are the creation and annihilation operators for Stokes, anti-Stokes, and phonon modes, respectively; $\omega_{\mathrm{s}j}$, $\omega_{\mathrm{a}j}$ and ω_{v} are their frequencies. The interaction with the multimode pump field is represented by the coupling constants $g_{\mathrm{s}j}$ and $g_{\mathrm{a}j}$ containing the field amplitudes. Frequencies and phases of the pump light are ω_{1j} and φ_{1j}, respectively.

The annihilation and creation operators fulfil the usual commutation relation

$$[a_j, a_k^{+}] = \delta_{jk} , \tag{2.2}$$

and the frequencies fulfil the resonant approximation conditions

$$\omega_{\mathrm{s}j} = \omega_{1j} - \omega_{\mathrm{v}} , \quad \omega_{\mathrm{a}j} = \omega_{1j} + \omega_{\mathrm{v}} . \tag{2.3}$$

From (2.1) and (2.2) we easily obtain the full set of the Heisenberg equations of motion

$$\dot{a}_{\mathrm{v}} = -\mathrm{i}\omega_{\mathrm{v}} a_{\mathrm{v}} + \sum_{j} \mathrm{i}[g_{\mathrm{s}j} a_{\mathrm{s}j}^{+} \mathrm{e}^{-\mathrm{i}(\omega_{1j}t - \varphi_{1j})} + g_{\mathrm{a}j}^{*} a_{\mathrm{a}j} \mathrm{e}^{\mathrm{i}(\omega_{1j}t - \varphi_{1j})}] ,$$

$$\dot{a}_{\mathrm{s}j} = -\mathrm{i}\omega_{\mathrm{s}j} a_{\mathrm{s}j} + \mathrm{i} g_{\mathrm{s}j} a_{\mathrm{v}}^{+} \mathrm{e}^{-\mathrm{i}(\omega_{1j}t - \varphi_{1j})} ,$$

$$\dot{a}_{\mathrm{a}j} = -\mathrm{i}\omega_{\mathrm{a}j} a_{\mathrm{a}j} + \mathrm{i} g_{\mathrm{a}j} a_{\mathrm{v}} \mathrm{e}^{-\mathrm{i}(\omega_{1j}t - \varphi_{1j})} , \tag{2.4}$$

which, after the substitution

$$a_j(t) = b_j(t)\,\mathrm{e}^{-\mathrm{i}\omega_j t}\,, \tag{2.5}$$

acquires the form

$$\begin{aligned}
\dot{b}_\mathrm{v} &= \mathrm{i}\sum_j [g_{\mathrm{s}j} b_{\mathrm{s}j}^+ \,\mathrm{e}^{\mathrm{i}\varphi_{1j}} + g_{\mathrm{a}j}^* b_{\mathrm{a}j}\,\mathrm{e}^{-\mathrm{i}\varphi_{1j}}]\,, \quad \dot{b}_\mathrm{v}^+ = (\dot{b}_\mathrm{v})^+\,,\\
\dot{b}_{\mathrm{s}j} &= \mathrm{i}g_{\mathrm{s}j} b_\mathrm{v}^+\,\mathrm{e}^{\mathrm{i}\varphi_{1j}}\,, \quad \dot{b}_{\mathrm{s}j}^+ = (\dot{b}_{\mathrm{s}j})^+\,,\\
\dot{b}_{\mathrm{a}j} &= \mathrm{i}g_{\mathrm{a}j} b_\mathrm{v}\,\mathrm{e}^{\mathrm{i}\varphi_{1j}}\,, \quad \dot{b}_{\mathrm{a}j}^+ = (\dot{b}_{\mathrm{a}j})^+\,.
\end{aligned} \tag{2.6}$$

To obtain the solution for b_j we rewrite (2.6) into a matrix equation and perform its Laplace transformation. It is convenient in the transformed matrix equation to arrange the row of transformed b_j into the following succession: b_v, b_v^+, $b_{\mathrm{s}1}$, $b_{\mathrm{s}1}^+$, $b_{\mathrm{a}1}$, $b_{\mathrm{a}1}^+$, $b_{\mathrm{s}2}$, $b_{\mathrm{s}2}^+$, $b_{\mathrm{a}2}$, $b_{\mathrm{a}2}^+$, ... Then calculation of the inverse matrix can be easily performed and the result has the form of sums analogous to (2.6). After the inverse Laplace transformation and the substitution (2.5), we have

$$\begin{aligned}
a_\mathrm{v}(t) &= a_\mathrm{v}(0)\,\vartheta + \sum_n [a_{\mathrm{s}n}^+(0)\,V_{\mathrm{s}n} + a_{\mathrm{a}n}(0)\,V_{\mathrm{a}n}]\,,\\
a_{\mathrm{s}n}(t) &= a_\mathrm{v}^+(0)\,G_n + \sum_m [a_{\mathrm{s}m}(0)\,S_{\mathrm{s}m} + a_{\mathrm{a}m}^+(0)\,S_{\mathrm{a}m}]\,K_{\mathrm{s}n} + a_{\mathrm{s}n}(0)\,\mathscr{S}_n\,,\\
a_{\mathrm{a}n}^+(t) &= a_\mathrm{v}^+(0)\,H_n + \sum_m [a_{\mathrm{s}m}(0)\,A_{\mathrm{s}m}^* + a_{\mathrm{a}m}^+(0)\,A_{\mathrm{a}m}^*]\,K_{\mathrm{a}n}^* + a_{\mathrm{a}n}^+(0)\,\mathscr{A}_n^*\,.
\end{aligned} \tag{2.7}$$

Here it holds that $a_j^+(t) = (a_j(t))^+$, so that we present for each mode only one operator $a_i(t)$ or $a_i^+(t)$. The coefficients are

$$\begin{aligned}
V_{\mathrm{s}n} &= \frac{\mathrm{i}}{\Omega}\,g_{\mathrm{s}n}\sin(\Omega t)\,\mathrm{e}^{-\mathrm{i}(\omega_\mathrm{v} t - \varphi_{1n})}\,, \quad \vartheta = \mathrm{e}^{-\mathrm{i}\omega_\mathrm{v} t}\cos(\Omega t)\,,\\
V_{\mathrm{a}n} &= \frac{\mathrm{i}}{\Omega}\,g_{\mathrm{a}n}^*\sin(\Omega t)\,\mathrm{e}^{-\mathrm{i}(\omega_\mathrm{v} t + \varphi_{1n})}\,,\\
G_n &= \frac{\mathrm{i}}{\Omega}\,g_{\mathrm{s}n}\sin(\Omega t)\,\mathrm{e}^{-\mathrm{i}(\omega_{\mathrm{s}n} t - \varphi_{1n})}\,, \quad \mathscr{S}_n = \mathrm{e}^{-\mathrm{i}\omega_{\mathrm{s}n} t}\,,\\
H_n &= \frac{-\mathrm{i}}{\Omega}\,g_{\mathrm{a}n}^*\sin(\Omega t)\,\mathrm{e}^{-\mathrm{i}(\omega_{\mathrm{a}n} t + \varphi_{1n})}\,, \quad \mathscr{A}_n = \mathrm{e}^{\mathrm{i}\omega_{\mathrm{a}n} t}\,,\\
K_{\mathrm{s}n} &= \frac{g_{\mathrm{s}n}}{\Omega^2}\,\mathrm{e}^{-\mathrm{i}(\omega_{\mathrm{s}n} t - \varphi_{1n})}\,[1 - \cos(\Omega t)]\,,\\
K_{\mathrm{a}n} &= \frac{-g_{\mathrm{a}n}}{\Omega^2}\,\mathrm{e}^{\mathrm{i}(\omega_{\mathrm{a}n} t + \varphi_{1n})}\,[1 - \cos(\Omega t)]\,,\\
S_{\mathrm{s}m} &= g_{\mathrm{s}m}^*\,\mathrm{e}^{-\mathrm{i}\varphi_{1m}}\,, \quad S_{\mathrm{a}m} = g_{\mathrm{a}m}\,\mathrm{e}^{\mathrm{i}\varphi_{1m}}\,, \quad A_{\mathrm{s}m} = S_{\mathrm{s}m}^*\,, \quad A_{\mathrm{a}m} = S_{\mathrm{a}m}^*\,,
\end{aligned} \tag{2.8}$$

where

$$\Omega^2 = \sum_n (|g_{\mathrm{a}n}|^2 - |g_{\mathrm{s}n}|^2)\,. \tag{2.9}$$

From the commutation relations (2.2), holding for all times, and (2.7) we obtain the identities

$$|\vartheta|^2 - \sum_n (|V_{sn}|^2 - |V_{an}|^2) = 1\,, \tag{2.10}$$

$$-|G_n|^2 + |K_{sn}|^2 \sum_m (|S_{sm}|^2 - |S_{am}|^2) + (S_{sn} K_{sn} \mathscr{S}_n + \text{c.c.}) = 0\,,$$

$$|H_n|^2 - |K_{an}|^2 \sum_m (|A_{sm}|^2 - |A_{am}|^2) + (A_{an} K_{an} \mathscr{A}_n^* + \text{c.c.}) = 0\,.$$

3. Antinormal and normal characteristic functions

We can examine statistical properties of the solution (2.7), at least in some limits. We will find the complete antinormal characteristic function defined by the formula [11]

$$\begin{aligned} C_{\mathscr{A}}(\beta_v, \beta_{si}, \beta_{ai}, t) &= \mathrm{Tr}\,\{\varrho(0) \exp[-\beta_v^* a_v(t)] \exp[-\beta_{s1}^* a_{s1}(t)] \\ &\times \exp[-\beta_{s2}^* a_{s2}(t)] \ldots \exp[-\beta_{a1}^* a_{a1}(t)] \exp[-\beta_{a2}^* a_{a2}(t)] \ldots \\ &\times \ldots \exp[\beta_{a2} a_{a2}^+(t)] \exp[\beta_{a1} a_{a1}^+(t)] \ldots \exp[\beta_{s2} a_{s2}^+(t)] \\ &\times \exp[\beta_{s1} a_{s1}^+(t)] \exp[\beta_v a_v^+(t)]\}\,. \end{aligned} \tag{3.1}$$

Here $a(t)$, $a^+(t)$ is the solution of the Heisenberg equations (2.7). It is necessary to reorder antinormally the operators $a_i(0)$ and $a_i^+(0)$ in (3.1) to the chosen order v, si, ai.

Let us shortly mention how different frequencies of s or a modes can be appreciated from the trace (3.1). In the following paragraphs we retract from the time dependent terms in $a_j(t)$ their high frequency dependence. This can be done when (3.1) is transformed toward the interaction picture. But when the frequencies of s or a modes are different we easily find that terms with the difference of frequencies $\omega_{s1} - \omega_{sj}$, $\omega_{a1} - \omega_{aj}$ must appear in the exponential terms of (3.1). This fact is omitted in the following.

We employ the Baker-Hausdorff theorem

$$\begin{aligned} &\exp(A + B) = \exp(A) \exp(B) \exp\{-[A, B]/2\} = \\ &= \exp(B) \exp(A) \exp\{[A, B]/2\}\,, \end{aligned} \tag{3.2}$$

where A, B are noncommuting operators fulfilling

$$[B, [A, B]] = [A, [A, B]] = 0\,.$$

Since the trace in (3.1) is a coherent-state trace, we can replace the operators $a_i(0)$ and $a_i^*(0)$ by c-numbers α_i and α_i^*, respectively [12]. Similarly we substitute the density matrix $\varrho(0)$ by $\langle \alpha_v, \alpha_{si}, \alpha_{ai} | \varrho(0) | \alpha_v, \alpha_{si}, \alpha_{ai} \rangle = \phi_{\mathscr{A}} \pi^3$, where $\phi_{\mathscr{A}}$ is the antinormal quasidistributions [11]. As the initial states we use a coherent state for the phonon

mode and displaced and squeezed states for the scattered modes. The resulting complete $\phi_{\mathscr{A}}$ reads (see the second work from [3])

$$\phi_{\mathscr{A}}(\alpha_v, \alpha_{si}, \alpha_{ai}) = \frac{1}{\pi} \exp\left(-\lambda_0 |\alpha_v - \xi_v|^2\right) \prod_i \left(\frac{1}{\mu_{si}\mu_{ai}\pi^2}\right)$$
$$\times \exp\left\{-|\alpha_{si} - \xi_{si}|^2 - \left[(v/2\mu)^*_{si}(\alpha_{si} - \xi_{si})^2 + \text{c.c.}\right]\right\}$$
$$\times \exp\left\{-|\alpha_{ai} - \xi_{ai}|^2 - \left[(v/2\mu)^*_{ai}(\alpha_{ai} - \xi_{ai})^2 + \text{c.c.}\right]\right\}, \tag{3.3}$$

where ξ means the coherent shift and v, μ are the squeezing parameters [13]. The parameter λ_0 in (3.3), which is finally set equal to 1, can be employed to prepare the phonon mode in a displaced Fock state mixed with noise at the beginning [14].

Now we can perform the trace summation in (3.1). It is replaced by the integration

$$C_{\mathscr{A}}(\beta_v, \beta_{si}, \beta_{ai}, t) = \int \phi_{\mathscr{A}}(\alpha_v, \alpha_{si}, \alpha_{ai}) \exp\left\{\alpha_v \lambda_v^* - \alpha_v^* \lambda_v\right\}$$
$$\times \prod_i \exp\left\{\alpha_{si}\lambda_{si}^* - \alpha_{si}^*\lambda_{si}\right\} \exp\left\{\alpha_{ai}\lambda_{ai}^* - \alpha_{ai}^*\lambda_{ai}\right\} \exp\left\{R\right\} \mathrm{d}^2\alpha_v \, \mathrm{d}^2\alpha_{si} \, \mathrm{d}^2\alpha_{ai}, \tag{3.4}$$

where $\phi_{\mathscr{A}}$ is from (3.3) and the exponential terms resulted from the reordering of the exponential terms in (3.1). The parameters are

$$\lambda_v^* = -\beta_v^* \vartheta + \sum_i (\beta_{si} G_i^* - \beta_{ai}^* H_i^*),$$
$$\lambda_{si}^* = -\beta_{si}^* \mathscr{S}_i - S_{si} \sum_j \beta_{sj}^* K_{sj} + A_{si}^* \sum_j \beta_{aj} K_{aj}^* + \beta_v V_{si}^*,$$
$$\lambda_{ai}^* = -\beta_{ai}^* \mathscr{A}_i - A_{ai} \sum_j \beta_{aj}^* K_{aj} + S_{ai}^* \sum_j \beta_{sj} K_{sj}^* - \beta_v^* V_{ai}. \tag{3.5}$$

Performing the integration in (3.4), the final expression for $C_{\mathscr{A}}$ is

$$C_{\mathscr{A}}(\beta_v, \beta_{si}, \beta_{ai}, t) = \left[\lambda_0 \prod_i |\mu_{si}\mu_{ai}| \sqrt{(\mathscr{K}_{si}\mathscr{K}_{ai})}\right]^{-1}$$
$$\times \exp\left\{R + R_v + \sum_i (R_{si} + R_{ai})\right\} \exp\left\{\frac{1}{\lambda_0}(\lambda_0 \xi_v - \lambda_v)(\lambda_0 \xi_v^* + \lambda_v^*)\right\}$$
$$\times \prod_i \exp\left\{\frac{1}{\mathscr{K}_{si}}\left[D_{si} D_{si}^1 - \left[(v/2\mu)^*_{si} D_{si}^2 + (v/2\mu)_{si} D_{si}^{12}\right]\right]\right\}$$
$$\times \exp\left\{\frac{1}{\mathscr{K}_{ai}}\left[D_{ai} D_{ai}^1 - \left[(v/2\mu)^*_{ai} D_{ai}^2 + (v/2\mu)_{ai} D_{ai}^{12}\right]\right]\right\}, \tag{3.6}$$

where the coefficients are

$$D_j = \xi_j + (v/\mu)_j \xi_j^* - \lambda_j, \quad D_j^1 = \xi_j^* + (v/\mu)_j^* \xi_j + \lambda_j^*,$$
$$K_v = \lambda_0^2, \quad \mathscr{K}_j = 1 - |v/\mu|_j^2, \quad R_v = -\lambda_0 |\xi_v|^2,$$
$$R_j = -|\xi_j|^2 - \left[(v/2\mu)_j^* \xi_j^2 + \text{c.c.}\right]; \quad (j = si, ai) \tag{3.7}$$

and

$$R = -[(\sum_i \beta_{ai}^* H_i^*)(\sum_j \beta_{sj}^* G_j) + \text{c.c.}] + |\sum_i \beta_{si}^* G_i|^2$$
$$- \{\beta_v^* [(\sum_n V_{sn} S_{sn})(\sum_i \beta_{sj}^* G_j) + \sum_i \beta_{si}^* V_{si} \mathscr{S}_i] + \text{c.c.}\}$$
$$+ \sum_n |\beta_v V_{sn}^* + A_{sn}^* \sum_i \beta_{ai} K_{ai}^*|^2 + |\sum_i \beta_{si}^* K_{si}|^2 \sum_m |S_{am}|^2$$
$$- \{\sum_m S_{am} [A_{am} \sum_j \beta_{aj}^* K_{aj} + \mathscr{A}_m \beta_{am}^*] [(\sum_i \beta_{si}^* K_{si}) + \text{c.c.}\} . \tag{3.8}$$

Here c.c. means complex conjugation of the previous term and in (3.4) we employed the following integral [15]

$$\int \exp [-B|\beta|^2 + (C/2)\beta^{*2} + (C_1/2)\beta^2 + D_1\beta + D\beta^*] \, \mathrm{d}^2\beta =$$
$$= \frac{\pi}{\sqrt{K}} \exp \left\{ \frac{1}{K} [DD_1 B + D^2(C_1/2) + D_1^2(C/2)] \right\},$$
$$K = B^2 - CC_1 , \quad \mathrm{Re}\, K > 0 , \quad \mathrm{Re}\, [B + (C_1 + C)/2] > 0 . \tag{3.9}$$

If we use the formula $|\mu|^2 - |v|^2 = 1$, holding for the parameters μ, v of squeezed light [13], the prefactor in (3.6) cancels itself and the term $1/\lambda_0$ remains.

The normal characteristic function $C_{\mathscr{N}}$ [11] can be expressed in terms of $C_{\mathscr{A}}$:

$$C_{\mathscr{N}}(\beta_v, \beta_{si}, \beta_{ai}) = C_{\mathscr{A}}(\beta_v, \beta_{si}, \beta_{ai}) \exp \{|\beta_v|^2 + \sum_i (|\beta_{si}|^2 + |\beta_{ai}|^2)\} . \tag{3.10}$$

This will be used in the subsequent sections.

4. Generating functions, photon-number distributions and factorial moments

Here we will investigate the single-mode factorial moments and the photon number distributions of the phonon and the scattered modes. We can calculate the single-mode generating function $C_{\mathscr{N}}^{(w)}$ [11]

$$C_{\mathscr{N}}^{(w)}(\lambda) = \frac{1}{\pi\lambda} \int \exp(-|\beta|^2/\lambda) \, C_{\mathscr{N}}(\beta) \, \mathrm{d}^2\beta , \tag{4.1}$$

where $C_{\mathscr{N}}$ is from (3.10) In this $C_{\mathscr{N}}$ we must set $\beta_i = 0$ for all β_i with the exception of β for the examined mode. For compound $C_{\mathscr{N}}^{(w)}$, $|\beta|^2$ in (4.1) should be replaced by the sum of $|\beta_i|^2$ over the calculated modes. It is still necessary to replace the prefactor $1/\pi\lambda$ in (4.1) by its n-th power, where n is the number of modes in the previous sum.

The generating function $C_{\mathscr{N}}^{(w)}$ generates factorial moments $\langle W^k \rangle_{\mathscr{N}}$ and photon number distributions $p(n)$ by [11]

$$\langle W^k \rangle_{\mathscr{N}} = (-1)^k \frac{\mathrm{d}^k}{\mathrm{d}\lambda^k} C_{\mathscr{N}}^{(w)}(\lambda)\big|_{\lambda=0}, \tag{4.2}$$

$$p(n) = \frac{(-1)^n}{n!} \frac{\mathrm{d}^n}{\mathrm{d}\lambda^n} C_{\mathscr{N}}^{(w)}(\lambda)\big|_{\lambda=1}. \tag{4.3}$$

In the following paragraphs we demonstrate that, in the single-mode case, both $\langle W^k \rangle_{\mathscr{N}}$ and $p(n)$ retain the same form, with different coefficients, for all modes v, *si*, a*i*. The items (i), (ii) and (iii) correspond to the phonon mode, the Stokes and the anti-Stokes modes, respectively.

(**i**) First we examine the phonon mode. Calculation of the integral (4.1) for $\beta = \beta_v$ can be performed with the help of the formula (3.9). Many terms cancel in the course of the integration. These are R_v, R_{si}, R_{ai} from (3.7) with the resident term from the integration, appearing in the exponent. As a result $C_{\mathscr{N}}^{(w)}$ acquires the form (3.9), multiplied by $1/\pi\lambda\lambda_0$. The coefficients B, C, C_1, D, D_1 are related by

$$B = B_0 + \frac{1}{\lambda}, \quad C_1 = C^*, \quad D_1 = -D^*, \tag{4.4}$$

where

$$\begin{aligned} B_0 &= -1 + \frac{|\vartheta|^2}{\lambda_0} + \sum_i \left[|V_{si}|^2 \left(\frac{1}{\mathscr{K}_{si}} - 1 \right) + |V_{ai}|^2 \frac{1}{\mathscr{K}_{ai}} \right], \\ C &= -\sum_i \left[(\nu/2\mu)_{si}^* \frac{V_{si}^2}{\mathscr{K}_{si}} + (\nu/2\mu)_{ai} \frac{V_{ai}^2}{\mathscr{K}_{ai}} \right], \\ D &= -\vartheta\, \xi_v - \sum_i (V_{si}\xi_{si}^* + V_{ai}\xi_{ai}). \end{aligned} \tag{4.5}$$

The parameters V_{si}, V_{ai}, ϑ and $\mathscr{K}_j$ are defined in (2.8) and (3.7), respectively.

We can further rewrite $C_{\mathscr{N}}^{(w)}$ into the form of a generating function for the Laguerre polynomials [11]

$$C_{\mathscr{N}}^{(w)} = \frac{1}{\lambda_0(1 - \lambda/\lambda_1)(1 - \lambda/\lambda_2)} \exp\left\{ \frac{\lambda\tau_1}{1 - \lambda/\lambda_1} + \frac{\lambda\tau_2}{1 - \lambda/\lambda_2} \right\}, \tag{4.6}$$

where the coefficients X, Y, Z, $\lambda_{1,2}$, $\tau_{1,2}$ are

$$\begin{aligned} X &= -B_0|D|^2 + D^2 \frac{C}{2} + \text{c.c.}., \quad Y = -B_0, \quad Z = |C|^2, \quad \lambda_{1,2} = \frac{1}{Y \pm \sqrt{Z}}, \\ \tau_1 &= \frac{\lambda_1 X - |D|^2}{1 - \lambda_1/\lambda_2}, \quad \tau_2 = \frac{\lambda_2 X - |D|^2}{1 - \lambda_2/\lambda_1}. \end{aligned} \tag{4.7}$$

In (4.6) we can use the parameter λ_0 to prepare the phonon mode in a displaced Fock state with noise [14]. For a coherent state, which is the case of this work, we

simply put $\lambda_0 = 1$. Inserting (4.6) into (4.2) and (4.3) we can obtain the photon number distributions p(n) and the factorial moments $\langle W^k \rangle_{\mathscr{N}}$ for the phonon mode [11, 14]

$$p(n) = \frac{(-4)^n}{\lambda_0} (EF)^{-1/2} (1 - 1/F)^n \exp(\tau_1/E + \tau_2/F) \sum_{i=0}^{n} \frac{1}{i!\,(n-i)!}$$

$$\times \left(\frac{1 - 1/E}{1 - 1/F}\right)^i H_{2i}\left[\sqrt{\frac{\tau_1}{E(E-1)}}\right] H_{2(n-i)}\left[\sqrt{\frac{\tau_2}{F(F-/1)}}\right], \tag{4.8}$$

$$\langle W^k \rangle = \frac{k!\,(F-1)^k}{\lambda_0} \sum_{i=0}^{k} \frac{(-4)^i}{i!\,(k-i)!} \left(\frac{E-1}{F-1}\right)^i$$

$$H_{2i}(\sqrt{-\lambda_1\tau_1})\, H_{2(k-i)}(\sqrt{-\lambda_2\tau_2})\,. \tag{4.9}$$

The coefficients E, F are defined by $E = 1 - 1/\lambda_1$, $F = 1 - 1/\lambda_2$. In (4.9) we have used a relation between the Hermite and the Laguerre polynomials [11].

In Sec. 6 we numerically investigate the factorial moments from (4.9)). The photon-number distribution $p(n)$ in (4.8) can be studied similarly. But from its structure we see that it corresponds to a simply displaced and squeezed vacuum field mixed with noise (see [14] and the form of $\phi_{\mathscr{A}}$ below).

(ii) For the Stokes field with the index i, the same integration must be performed as for the phonon mode. The integration parameter in (4.1) is $\beta = \beta_{si}$. Again many terms cancel and the resulting generating function $C_{\mathscr{N}}^{(w)}$ acquires the same form as for the phonon mode. The new coefficients follow

$$B_0 = -1 + |K_{si}|^2 \sum_j \left[|S_{sj}|^2 \frac{1}{\mathscr{K}_{sj}} + |S_{aj}|^2 \left(\frac{1}{\mathscr{K}_{aj}} - 1\right)\right]$$

$$+ \frac{1}{\mathscr{K}_{si}} \left[1 + (\mathscr{S}_i^* S_{si} K_{si} + \text{c.c.})\right] + \left(1 - \frac{1}{\lambda_0}\right) |G_i|^2\,,$$

$$C = -K_{si}^2 \sum_j \left[(v/2\mu)_{sj} \frac{S_{sj}^2}{\mathscr{K}_{sj}} + (v/2\mu)_{aj}^* \frac{S_{aj}^2}{\mathscr{K}_{aj}}\right]$$

$$- \frac{1}{\mathscr{K}_{si}} \left[(v/2\mu)_{si} (\mathscr{S}_1^2 + 2\mathscr{S}_i S_{si} K_{si})\right],$$

$$D = -G_i \xi_v^* - K_{si} \sum_j (S_{sj}\xi_{sj} + S_{aj}\xi_{aj}^*) - \xi_{si}\,. \tag{4.10}$$

Here, S_j, G_j, $\mathscr{S}_j$ and $\mathscr{K}_j$ are from (2.8) and (3.7), respectively. The calculation of photon-number statistics and factorial moments is the same as for the phonon mode.

(**iii**) For the anti-Stokes field with the index i, the same holds as for the Stokes fields. The integration parameter in (4.1) is $\beta = \beta_{ai}$ and the constants B_0, C, D are

$$B_0 = -1 + |K_{ai}|^2 \sum_j \left[|A_{sj}|^2 \left(\frac{1}{\mathscr{K}_{sj}} - 1 \right) + |A_{aj}|^2 \frac{1}{\mathscr{K}_{aj}} \right] + \frac{|H_i|^2}{\lambda_0}$$

$$+ \frac{1}{\mathscr{K}_{ai}} \left[1 + (\mathscr{A}_i^* A_{ai} K_{ai} + \text{c.c.}) \right],$$

$$C = -K_{ai}^2 \sum_j \left[(\nu/2\mu)_{sj}^* \frac{A_{sj}^2}{\mathscr{K}_{sj}} + (\nu/2\mu)_{aj} \frac{A_{aj}^2}{\mathscr{K}_{aj}} \right]$$

$$- \frac{1}{\mathscr{K}_{ai}} \left[(\nu/2\mu)_{ai} (\mathscr{A}_1^2 + 2\mathscr{A}_{ia} A_{ai} K_{ai}) \right],$$

$$D = -H_i^* \xi_v - K_{ai} \sum_j (A_{sj} \xi_{sj}^* + A_{aj} \xi_{aj}) - \xi_{ai}. \tag{4.11}$$

Similarly as for the Stokes modes, the parameters A_j, H_j, $\mathscr{A}_j$ and $\mathscr{K}_j$ are from (2.8) and (3.7), respectively.

We notice that all exponentials from this paragraph, which strongly depend on time, can be replaced by 1. This follows from the fact that in the resonant case (and the same frequencies for s and a modes) they cancel.

The antinormal quasidistributions $\phi_{\mathscr{A}}$ for single modes can be found by the inverse Fourier transform of the antinormal characteristic function from (3.6). In this $C_{\mathscr{A}}$ we must set $\beta_j = 0$ for all modes excepting the studied one. The resulting $\phi_{\mathscr{A}}$ for the modes v, si, ai acquire the form (3.9) multiplied by the coefficient $1/\pi\lambda_0$. The parameters B', C', D' for the modes v, si and ai are expressed in the form of B_0, D, C, from (4.5), (4.10) and (4.11). These relations are $B' = B_0'$ (instead of $B = B_0 + 1/\lambda$), $B_0' = B_0 + 1$, $D' = D + \alpha$, $D_1' = -D'$, $C' = C$ and $C_1' = C^*$.

Combined cases (ss, sa, aa, sv, sa, sss, ...) can be investigated similarly as the single mode case [11]. Particularly we can study combined photon-number statistics and factorial moments (see [3]). We already described how a combined $C_{\mathscr{N}}^{(w)}$ can be found (below (4.1)). The resulting coefficients wouls be very complicated and an analysis could be quite similar to that performed by Kárská and Peřina [3].

5. Numerical results

We will give some numerical examples of factorial moments for the fields v, s, a. We confine our investigation to two pump, two Stokes, and two anti-Stokes fields. This case can be reasonably analysed numerically and we can observe interesting cooperative phenomena. We divide the investigation into several points (A–E), in which we successively connect scattering modes to the phonon mode, choosing the pertinent constants g_{si}, g_{ai} nonzero. From (2.9) it is clear that if the sum of $|g_{si}|^2$ is greater than that of $|g_{ai}|^2$, we obtain an imaginary frequency Ω. This coresponds

to the exponential growth of the amplitude of scattering modes. We will not study this problem and will consider only the case of a real frequency Ω. Then the described sums are in the reversed sequence of magnitudes.

Symmetries appearing in the Hamiltonian (2.1) simplify examination in the examples presented below. From the Hamiltonian (2.1) we can obtain some restrictions on independent phases. A great simplification arises if coherent states are in the input. Then all operators a_i, a_i^+ can be substituted by α, α^* (the same hold for a_i, a_i^+ in S matrix in a coherent state representation). In this case two series of relations follow from (2.1)

$$F_v + F_{sj} - F_{lj} = C_{sj}\,, \quad F_v - F_{aj} + F_{lj} = C_{aj}\,, \tag{5.1}$$

where phases F_v, F_{lj}, F_{sj}, F_{aj} are defined in Table 1. As a result we obtain the invariance of an evolution for various phases when C_{sj}, C_{aj} are unchanged. For squeezed states these symmetries hold with the restriction which we will describe now. Let us fix C_{sj}, C_{aj}. Then the phases F_v, F_{sj}, F_{aj} can be changed by rotating the initial states with the shifts m_j (see Table 1) in the complex plane α. Phases F_{lj} simply correspond to the classical light. To preserve invariance under (5.1) we must rotate the elliptical distributions $\phi_{\mathcal{A}}$, for the rotating initial squeezed states, around their centers at the same time (this holds for all $\phi_{\mathcal{A}}$ which are squeezed and whose phases F_i are varied). The inclination of the ellipses is described by the phases f_{sj}, f_{aj} (see Table 1). This rotation should be performed in the same sense with two times higher angular velocity. The rotating ellipse comes for the first time into itself when its angle f_j is changed by 2π.

Further symmetry of the solution lies in the product Ωt. It appears in the arguments of the sine and cosine in the solution of the Heisenberg equations (2.4). Pumps with sufficiently high intensities can be treated classically. For example for $\Omega \approx 10^7\ \mathrm{s}^{-1}$ [6] and $\Omega t = 1$ we obtain the time of evolution 10^{-7} s. In figures the parameter $t \in \langle 0, 3\rangle$ is assumed. The constants g_j are of the same magnitude. The transformation toward realistic times for a chosen g_i, if it is sufficiently large to describe classical light, can be performed easily.

Below we present two types of figures. The first type shows the reduced factorial moments (RFM) $\langle W^k\rangle_{\mathcal{N}}/\langle W\rangle_{\mathcal{N}} - 1$ with $k = 2 - 4$ for one or two modes. The second type gives the mean integrated intensity $\langle W\rangle$ or the second RFM for all modes in the studied point. We show only several typical examples and do not try to describe a complete behaviour of the modes. Since there are many parameters for every picture we summarize them in Table 1 and reference them as No. I, No. II,.... We use five types of lines. The phonon mode has a solid line. The first and second Stokes modes are represented by dotted and dashed lines, respectively. For the first and second anti-Stokes modes single and double dash-dotted lines are used, respectively. It seem that a rule holds which orders RFM for a given mode in figures. The RFM are ordered ($k = 2 - 4$) in the times of extremes of curves from the lower to the higher RFM with growing absolute values of the curves.

Table 1. Numerical parameters of modes.

No.	g_{s1} m_{s1} s_{s1}	g_{s2} m_{s2} s_{s2}	g_{a1} m_{a1} s_{a1}	g_{a1} m_{a2} s_{a2}	φ_{l1} F_{s1} f_{s1}	φ_{l2} F_{s2} f_{s2}	m_v F_{a1} f_{a1}	F_v F_{a2} f_{a2}
	0·01	0·01	0·01	2·00	0·00	0·40	1·00	0·00
I	0·01	0·01	0·01	2·00	0·00	0·00	0·00	0·00
	0·05	0·05	0·05	0·60	0·00	0·00	0·00	0·00
	0·01	0·01	1·50	2·00	0·00	1·57	1·50	0·00
II	0·01	0·01	2·00	3·00	0·00	0·00	0·00	0·00
	0·05	0·05	0·60	0·30	0·00	0·00	0·00	3·14
	0·01	0·01	1·70	2·00	0·00	0·00	1·50	0·00
III	0·01	0·01	2·00	3·00	0·00	0·00	0·00	0·00
	0·05	0·05	0·50	0·70	0·00	0·00	0·00	3·14
	0·01	1·00	0·01	3·00	0·00	0·50	1·50	0·00
IV	0·01	1·50	0·01	2·50	0·00	1·57	0·00	0·00
	0·05	0·05	0·05	0·60	0·00	3·14	0·00	0·00
	1·00	0·01	0·01	3·00	−1·00	0·50	1·50	0·00
V	1·50	0·01	0·01	2·50	1·57	0·00	0·00	0·00
	0·05	0·05	0·05	0·60	3·14	0·00	0·00	0·00
	1·00	1·00	3·00	3·00	0·00	1·57	1·50	1·57
VI	1·80	2·50	2·00	3·00	0·00	3·14	0·00	3·14
	0·40	0·50	0·40	0·70	3·70	0·00	3·14	0·30
	1·00	1·00	3·00	3·00	1·57	1·57	1·50	1·57
VII	1·80	2·50	2·00	3·00	0·00	3·14	0·00	3·14
	0·40	0·50	0·40	0·70	3·70	0·00	3·14	0·30
	1·00	1·00	3·00	3·00	3·14	1·57	1·50	1·57
VIII	2·50	1·50	2·50	3·00	3·14	3·14	3·14	2·50
	0·60	0·20	0·30	0·60	3·14	0·00	0·40	0·00

For the purpose of tabelation we define $\xi_j = m_j \exp(\mathrm{i}F_j)$, $\xi_v = m_v \exp(\mathrm{i}F_v)$ $(v/2\mu)_j = s_j \exp(\mathrm{i}f_j)$.

(A) First we set $g_{a2} \neq 0$ and $g_i = 0$ for all other g_i. This corresponds to the scattering of a single anti-Stokes mode.

In Fig. 1 we see the k-th RFM with $k = 2, 3, 4$ for the phonon and the second anti-Stokes modes. The parameters are in No. I. We observe that RFM for both modes are periodical. Particularly we can see a sub-poissonian behaviour at some times. This nonclassical phenomenon transforms itself from the anti-Stokes toward the phonon mode and back.

(B) Here we let $g_{ai} \neq 0$ for the two anti-Stokes modes and put $g_{si} = 0$ for the Stokes modes.

In Fig. 2 there is the mean integrated intensity for the phonon and the anti-Stokes modes, with the parameters in No. II. We can see that the phonon mode has harmonical $\langle W \rangle$, but the s, a modes have only periodical $\langle W \rangle$. This can be already expected from the solution (2.7). The period of the anti-Stokes modes is two times higher than that of the phonon mode. It seems that the sum of the anti-Stokes modes lies in the opposite phase to the phonon mode, similarly as in Fig. 1.

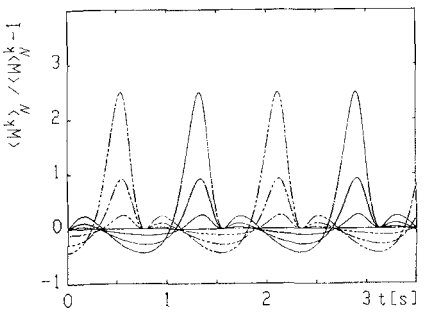

Fig. 1.

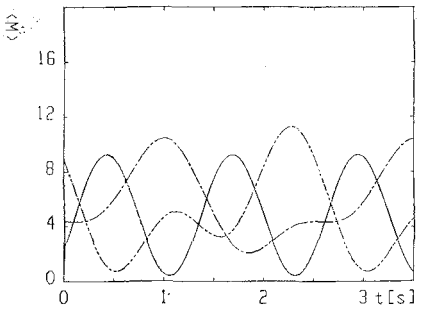

Fig. 2.

Fig. 1. Time evolution of the k-th RFM with $k = 2, 3, 4$ for the phonon and the second anti-Stokes modes. The parameters are in No. I of Table 1. Sub-poissonian behaviour appears periodically in both modes.

Fig. 2. Mean integrated intensity for the phonon and the two anti-Stokes modes with the constants in No. II. The phonon mode has harmonical $\langle W \rangle$, but the s, a modes have only periodical $\langle W \rangle$. The period of the anti-Stokes modes are two times higher than that of the phonon mode.

Figure 3 shows the same situation as Fig. 1 does, but for the two anti-Stokes modes. The parameters are as in Fig. 2. Here it is important to mention that the maxima in the k-th moments and $k > 2$ appear at the local minima of $\langle W \rangle$ for the given mode. This can also be expected from the definition of RFM. It is interesting that the mode with super-poissonian statistics (a_2) can acquire a sub-poissonian statistics in the course of evolution. This event can appear several times during one period.

Figure 4 is the continuation of Fig. 3 for the phonon mode. Here a very impressive behaviour of RFM around the minima of $\langle W \rangle$ can be seen for this mode. The leading slope grows monotonously and nearly linearly up to some maximum. Then a very narrow fall of noise comes. After this sub-poissonian minimum the RFM again quickly acquire the previous value for a short time.

In Fig. 5 we see the second RFM for the phonon and the anti-Stokes modes with parameters from No. III. One can observe interesting oscillation in the second RFM of the anti-Stokes modes. Since they are in opposite phases, we can presume that they correspond to some cooperative phenomenon in the two modes.

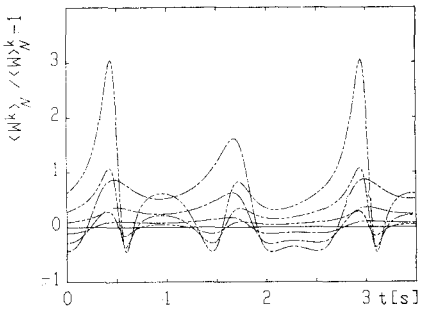

Fig. 3.

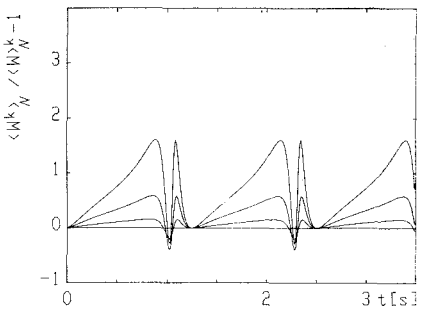

Fig. 4.

Fig. 3. Same as Fig. 1, but for the two anti-Stokes modes. The parameters are as in Fig. 2.The maxima in the k-th moments and $k > 2$ appear at the local minima of $\langle W \rangle$ for the given mode. The mode a2, having super-poissonian statistics at the beginning, can acquire periodically a sub-poissonian statistics in the course of evolution.

Fig. 4. Continuation of Fig. 3 for the phonon mode. Very narrow noise collapses can be observed around the minima of $\langle W \rangle$ for this mode. The curves grow nearly linearly in some time intervals and then abruptly fall to negative values. At these times the phonon mode has sub-poissonian statistics.

Figure 6 shows the detail of RFM for the second anti-Stokes mode and $k = 2 - 4$ from Fig. 5. We can observe that higher RFM look like a simple magnification of the lower RFM. Such narrow noise oscillations could be used for phase location applications.

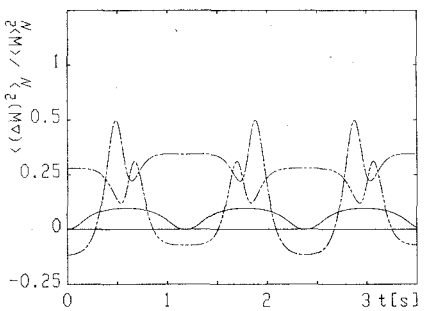

Fig. 5.

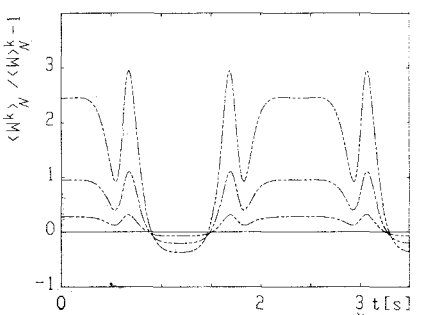

Fig. 6.

Fig. 5. The second RFM for the phonon and the anti-Stokes modes. The constants are from No. III. Typical noise oscillations are superimposed on the periodical curves. They appear with opposite phases in the two anti-Stokes modes and reveal some cooperative behaviour of the two modes.

Fig. 6. Detail of RFM for the second anti-Stokes mode and $k = 2-4$ from Fig. 5. Higher RFM look like a simple magnification of the lower RFM. The narrow noise oscillations could lead to new applications.

(C) Now we couple the Stokes modes to the phonon mode. First we let nonzero only the second Stokes and anti-Stokes modes.

In Fig. 7 we observe the second RFM for the phonon, the second Stokes and anti-Stokes modes with parameters from No. IV. We observe that the curves for the phonon and anti-Stokes modes are similar to those from Fig. 1. The anti-Stokes curve is rather deformed by the presence of the Stokes mode. This mode does not have a complicated behaviour.

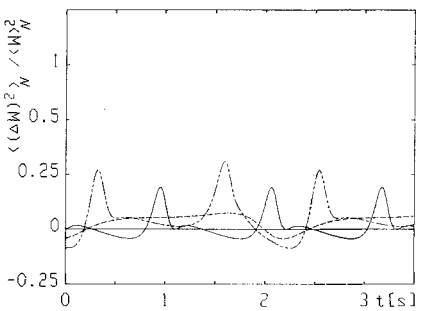

Fig. 7.

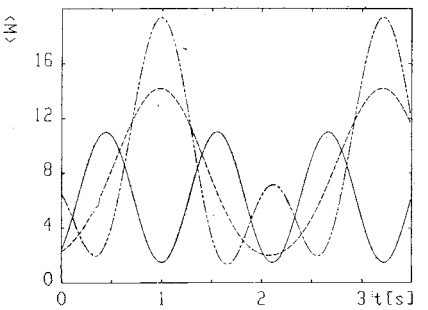

Fig. 8.

Fig. 7. The second RFM for the phonon, the second Stokes and anti-Stokes modes with parameters from No. IV. The phonon mode becomes squeezed in the course of evolution similarly as in Fig. 1. The presence of the Stokes mode changes the behaviour of the anti-Stokes mode.

Fig. 8. Mean integrated intensity for the same values and modes as in Fig. 7. The second anti-Stokes mode acquires rather large values and is not harmonical. The other two modes seem to be more regular.

Figure 8 shows the mean integrated intensity for the same values and modes as in Fig. 7. Again it can be seen that the anti-Stokes mode has the most complicated structure. It looks like to be formed from a superposition of two harmonics. But this is only a simplified view on the situation.

(D) In this point we use a different index for the Stokes and the anti-Stokes modes. This enables us to study anomalies observed when scattering modes with different indices are coupled to the phonon mode.

Figure 9 is analogous to Fig. 7 and corresponds to the parameters in No. V. The Stokes modes are exchanged and the parameters of the first pump and the Stokes modes are the same as in Fig. 7. Only the phase of the first pump field is different from that in Fig. 7. If the phases of the pump modes were the same, Fig. 9 would be identical to Fig. 7, but for the exchange of the Stokes modes. The Hamiltonian (2.1) can give yet another interpretation. Different phases of the pumps can be considered to be equivalent to making the constant g_{s2} of the mode s2 complex, and at the same time to neglecting the exchange of the Stokes modes. In Fig. 9 some noise expansion can be seen both in s and a modes.

In Fig. 10 there is the mean integrated intensity for the parameters from Fig. 9. We can see that the situation seems to be opposite when compared with Fig. 8, where large amplitudes were in $\langle W \rangle$ and small ones in the second RFM. Here the situation is opposite.

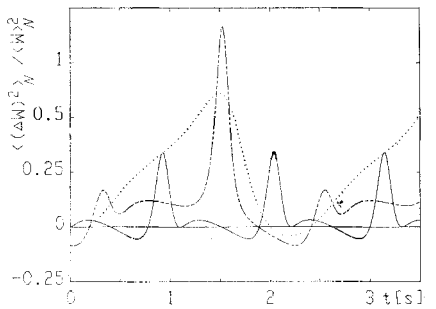

Fig. 9.

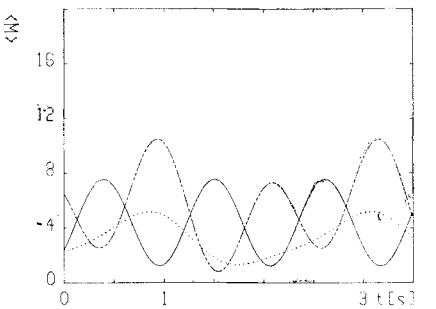

Fig. 10.

Fig. 9. As in Fig. 7, but for the parameters in No. V. Here the Stokes modes are exchanged and the phases of the two pump fields are different. We can see that this inequivalence of phases leads to sharp production of noise in one of the anti-Stokes modes at some times.

Fig. 10. As in Fig. 8, but with the constants from Fig. 9. Here the behaviour is much more regular than in Fig. 8. The roles of the mean integrated intensity and the second RFM in Figs. 7, 8 seem to be opposite to that in Figs. 9, 10. Here there are large amplitudes in RFM and small amplitudes in $\langle W \rangle$.

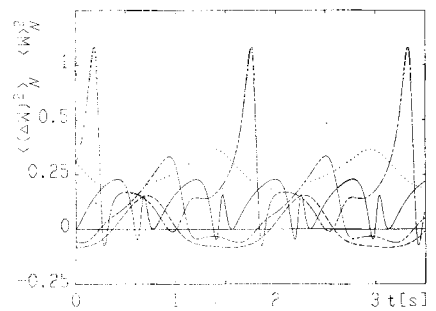

Fig. 11.

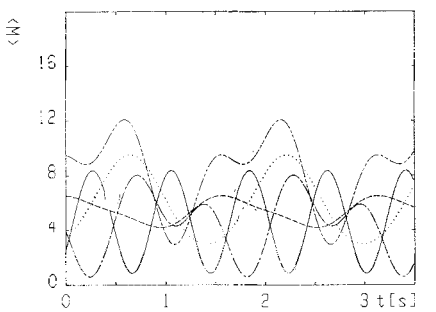

Fig. 12.

Fig. 11. The second RFM for all modes and parameters from No. VI. In the course of evolution some of the modes become sub- and other super-poissonian. Noise collapses follow noise expansions. Generally, the Stokes modes have simpler behaviour than the anti-Stokes modes.

Fig. 12. Mean integrated intensity for the parameters as in Fig. 11. We can observe that local minima occur simultaneously in both anti-Stokes modes. $\langle W \rangle$ for the phonon mode is harmonical but it is more complex for the other modes.

(E) Finally we study the general situation with all g_{ai} and g_{si} nonzero.

Figure 11 shows the second RFM for all the modes for parameters from No. VI. It is seen that in the full generality the situation becomes quite uneasy to survey. The curves are very structured. Particularly we see that they become sub-poissonian at some times. The Stokes modes are more elementary than the anti-Stokes modes.

In Fig. 12 there is the mean integrated intesity for the parameters as in Fig. 11. We can compare the phase relations of $\langle W \rangle$ for different modes and see how the first and the second RFM are correlated. $\langle W \rangle$ for the phonon mode is harmonical in all figures. The Stokes modes are again simpler than the anti-Stokes modes.

Figure 13 presents the same situation as Fig. 11 does, but the phases of the pumps have equal values (No. VII). We can observe that the curves are completely different in comparison with Fig. 11. Some deviation from harmonicity can be seen in the phonon mode. This is in contrast with the complex behaviour of the phonon mode in Fig. 11.

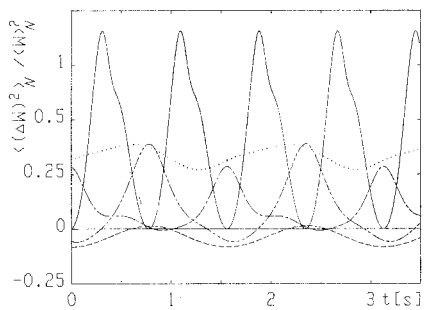

Fig. 13.

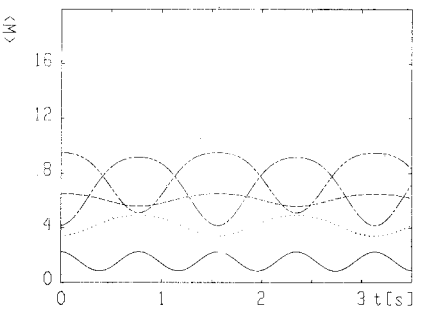

Fig. 14.

Fig. 13. Same as in Fig. 11, but the phases of the pumps have equal values. The parameters are in No. VII. Now, noise appears especially in the phonon mode. The dependence on the phases of the pumps is so strong that the curves are completely different from those in Fig. 11. Here they seem less structured.

Fig. 14. As in Fig. 12, but for the parameters from Fig. 13. Here the behaviour is much more regular than in Fig. 12. This reflects a strong dependence of the modes behaviour in the evolution on the phase of the pumps. Minima and maxima of the two anti-Stokes modes are in the counter-phase.

Figure 14 shows the mean integrated intensity for parameters in Fig. 13 and it is therefore the analog of Fig. 12. We can observe that, as for the second RFM, the curves are quite different from Fig. 12. This suggests that the behaviour of modes in the evolution is very dependent on the phase of the pumps. The dependence on parameters of any scattered mode (amplitude, phase, squeezing) is much weaker.

Figure 15 shows the second RFM for the constants from No. VIII. Similar comments as in Fig. 11 could be given here. The first anti-Stokes mode has an interesting

behaviour. In some moments its second RFM turns nearly at the right angle to the horizontal direction. The points of the phonon curve are interesting, too.

Finally, Fig. 16 is the detail of RFM with $k = 2 - 4$ for the Stokes modes. We see that the Stokes modes are generally less structured than the anti-Stokes modes. They have regular sub-super-poissonian behaviour.

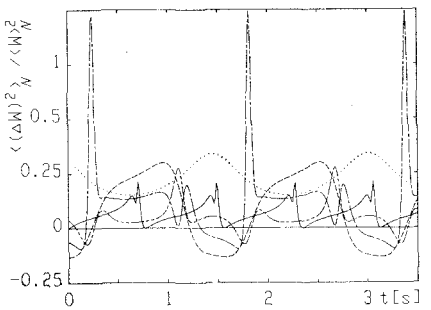

Fig. 15.

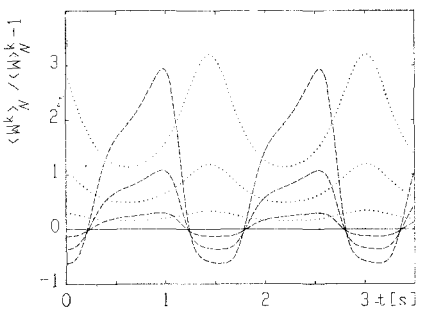

Fig. 16.

Fig. 15. The second RFM for the constants from No. VIII. A very irregular behaviour can be observed in the phonon and the first anti-Stokes modes at some times. This suggests that the Fourier resolution of these curves would give large components of higher harmonics.

Fig. 16. Detail of RFM with $k = 2-4$ for the Stokes modes for the parameters from Fig. 15. The curves have regular sub-super-poissonian behaviour. The mode which was super-poissonian at the beginning never becomes sub-poissonian for this choice of parameters.

To conclude this section we can say that the scattering with squeezed light has a number of anomalies. Particularly with a multimode pump the RFM and the mean integrated intensity of all modes become very complicated.

6. Conclusion

We have investigated stimulated Raman (Brillouin) scattering on the system which can be modelled as a one phonon mode. We have used a strong multimode pump light, described classically. The scattered modes were prepared in displaced and squeezed states and the phonon mode was in coherent state. As the result of the interaction interesting effects have been observed. We have found very irregular behaviour of RFM when several squeezed modes are coupled to the phonon mode. Particularly, the modes have periodical RFM at the chosen conditions and they can pass from super-poissonian statistics toward sub-poissonian ones.

The author would like to thank Dr. J. Peřina for fruitful discussions. and Dr. A. Lukš for comments on the results.

References

[1] Proc. of the Eleventh Inter. Conf. on Raman Spectroscopy, London (England), 5—9 Sept. 1988 (Eds. R. J. H. Clark, D. A. Long). J. Wiley & Sons, New York, 1988.
[2] Li Z. W., Radzewicz C., Raymer M. G.: J. Opt. Soc. Am. B *5* (1988) 2340.
[3] Peřina J.: Opt. Acta, *28* (1981) 325 and 1529.
Kárská M., Peřina J.: J. Mod. Opt. *37* (1990) 195.
[4] Shen Y. R.: The Principles of Nonlinear Optics. J. Wiley & Sons, New York, 1984.
[5] Benivegna G., Messina A.: Phys. Rev. A *37* (1988) 4747.
Xu Lun-Bia, Cai Shou-Fu, Xie Guo-Xin: Phys. Status Solidi B *150* (1988) 797.
[6] Pieczonková A., Peřina J.: Czech. J. Phys. B *31* (1981) 837.
Pieczonková A.: Czech. J. Phys. B *32* (1982) 831; Opt. Acta *29* (1982) 1509; Czech. J. Phys. B *33* (1983) 923.
[7] Holtz H., Venkateswaran U. D., Syassen K., Ploog K.: Phys. Rev. B *39* (1988) 8458.
Suh E.-K. et al.: Phys. Rev. B *36* (1987) 4316.
[8] Georges A. T.: Phys. Rev. A *39* (1989) 1876, and references therein.
[9] de Oliveira F. A. M., Knight P. L.: Phys. Rev. Lett. *7* (1988) 830.
[10] Ritsch H., Zoller P.: Phys. Rev. Lett. *9* (1988) 1097.
[11] Peřina J.: Quantum Statistics of Linear and Nonlinear Optical Phenomena. D. Reidel, Dordrecht—Boston, 1984.
Glauber R. J.: Quantum Optics (Eds. Kay S. M., Maitland A.). Academic Press, London, 1970.
[12] Louisell W. H.: Quantum Statistical Properties of Radiation. J. Wiley & Sons, New York, 1973.
[13] Yuen H. P.: Phys. Rev. A *13* (1976) 2226.
[14] Král P.: J. Mod. Opt. *37* (1990) 889.
Král P.: Kerr Interaction with Displaced and Squeezed Fock states (to be published in Phys. Rev. A).
[15] Peřinová V.: Optica Acta *28* (1981) 747.